Physica Status Solidi -Rapid research letters, p.1800445, 2019.
https://doi.org/10.1002/pssr.201800445

Transmission microsphere-assisted dark-field microscopy

Stephane Perrin[*,1], Hongyu Li[1], Keshia Badu[1], Thomas Comparon[1], Giorgio Quaranta[2,3], Nadia Messaddeq[4], Nicolas Lemercier[4], Paul Montgomery[1], Jean-Luc Vonesch[4], Sylvain Lecler[1]

[1] ICube laboratory, UMR CNRS 7357 - University of Strasbourg, 67412 Illkirch, France
[2] CSEM SA, Tramstrasse 99, 4132 Muttenz, Switzerland
[3] EPFL Lausanne, Nanophotonics and Metrology Laboratory, 1015 Lausanne, Switzerland
[4] IGBMC institute, UMR CNRS 7104 - INSERM - University of Strasbourg, 67404 Illkirch, France

Key words: Microsphere-assisted microscopy, Dark-field imaging, Optical super-resolution, Translucent medium imaging.

[*] Corresponding author: stephane.perrin@unistra.fr

Microsphere-assisted microscopy allows the limit of the diffraction of light to be overcome while being non-invasive, full-field, label-free and easy-to-implement. However, the observation of translucent samples remains difficult using a classical bright-field illumination. In this work, a method is presented for the inspection of quasi-transparent sub-diffraction-limited structures by using dark-field illumination in the transmission mode. Glass-imprint features, having a size of 250 nm, as well as fixed mouse brain cells have been visualized using the dark-field microsphere-assisted technique. The possibility to observe feature sizes up to 100 nm has been demonstrated in air using a 25-μm-diameter glass microsphere combined with an optical microscope, opening new possibilities for biological imaging.

Introduction In optical microscopy, imaging sub-micrometre features is still a real challenge. In fact, the resolving power in classical white-light microscopy is limited by the diffraction of light, resulting in the smallest discernible size of $\lambda/2$ (where λ is the wavelength of light) using an aberration-free imaging system having a unit numerical aperture [1,2]. Since 1928 when the notion of *ultramicroscopy* appeared [5], several approaches have thus been purposed in order to overcome this physical barrier [3] such as (listed in chronological order) scanning near-field optical microscopy [6], *superlenses* based on negative-refractive-index materials [7,8,9] or structured illumination microscopy [10,11]. Afterwards, confocal microscopy, known through M. Minsky's patent [12] despite its principle being previously revealed [13,14], made it possible to reach a few hundred nanometres in lateral resolution. 4Pi microscopy [15] and photonic-jet-based scanning microscopy [16] have further enhanced confocal microscopy performance. In 2014, advances in optical nanoscopy were rewarded by the Nobel Prize for Chemistry through super-resolved fluorescence microscopy and single molecule localization microscopy [4]. However, these techniques are often photo-toxic for the sample, are complex to implement, need markers or require long-acquisition times.

In 2011, Z. Wang *et al.* experimentally demonstrated the principle of full-field sub-diffraction-limit microscopy by only introducing glass microspheres inside a classical microscope [17]. This easy-to-implement and non-invasive white-light nanoscopy technique allows the diffraction limit to be overcome by a factor of 2 ($\lambda/4$) [18] to 3 ($\lambda/6$) [19]. Through a probable conversion of the near-field information to propagating waves [20], microsphere-assisted microscopy is thus able to achieve a lateral resolution that is superior to that attainable by confocal microscopy and by the solid immersion lens [21], and similar to that achieved from structured illumination microscopy and meta-material-based *superlenses*. Moreover, microsphere-assisted microscopy has recently been adapted to fluorescence microscopy [22,23] and to interference microscopy [24,25,26]. However, the label-free visualization of transparent objects still remains difficult such as in classical microscopy. The unscattered light from these types of ob-

jects indeed reduces the imaging contrast, rendering the features imperceptible.

In microsphere-aided microscopy, up until now, dark-field illumination has only been applied in the reflection mode to enhance the imaging contrast of opaque objects [27]. In this letter, the interest and the specificity of dark-field nanoscopy in the transmission mode is demonstrated for the direct imaging of fully-translucent samples (*e.g.* biological elements) having detail sizes of a few hundred nanometres. First, the phenomenon of super-resolution microscopy is shown by retrieving the transfer function of the microsphere-based system. Then, nano-imprint glass random features and mouse brain cells were measured, highlighting the principle of transparent-object imaging.

Methods A commercial optical microscope (Axio Scope A1, Zeiss) using dark-field illumination in the transmission mode has been adapted for super-resolution microscopy using microspheres. As illustrated in Fig. 1(a), the incident beam from the Köhler-arranged light source is first spatially modified using a ring mask in order to illuminate the sample with a hollow cone of light by passing through the condenser lens. In dark-field microscopy, only the light diffracted or scattered by the sample (represented in blue color in Fig. 1(a)) enters the imaging part where the microscope objective ($\times$20, NA = 0.4, Zeiss) is represented. As the condenser lens has a numerical aperture (NA = 0.8) that is higher than the microscope objective, the direct transmitted beam (represented in red color in Fig. 1(a)) is not recorded and thus not considered in the image formation. A soda-lime-glass microsphere with a diameter of 25 µm (SLGMS, Cospheric) is inserted between the microscope objective and the sample to be tested, giving a magnified virtual image (with, here, $\gamma \sim 5$). This arrangement allows the light scattered by sub-diffraction-limit features to be collected by the microscope objective which finally directs the virtual image onto the camera (AxioCam, Zeiss).

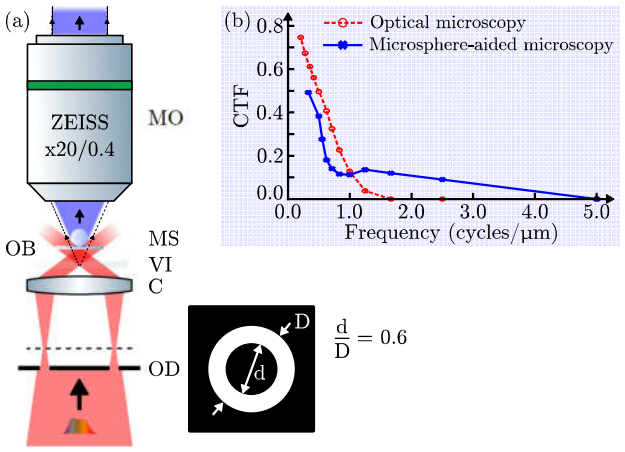

Figure 1 Dark-field microsphere-assisted microscope. (a) Layout of the imaging system. The incident beam from the white-light source (in red) is spatially blocked by the obstruction disk (OD) and focused by the condenser lens (C) to illuminate the object (OB). A glass microsphere (MS), placed on the OB surface, collects the light scattered by the OB features (in blue) and generates a super-resolved virtual image (VI) below the OB plane. A microscope objective (MO) finally directs the VI into the imaging part of the microscope. (b) Contrast transfer function (CTF) comparison of the optical microscope with and without the microsphere in the transmission mode. The cut-off frequencies of the microscope and the nanoscope are 1.278 µm^{-1} and 5.068 µm^{-1}, respectively.

The performance of the transmission optical nanoscope has been first estimated by characterizing its resolving power. Figure 1(b) shows the contrast transfer function of the imaging system as a function of the frequency of a periodic signal [2]. The cut-off frequency of the microscope alone reaches 1.278 µm^{-1} and is thus only able to resolve 800-nm-period features. Microsphere-assisted microscopy makes it possible, in this case, to increase the resolution limit by a factor of 4.0, *i.e.* enabling the visualization of features having a period as small as around 200 nm, *i.e.* features having a size as small as 100 nm. An equivalent numerical aperture of 1.5 is achieved which is around twice the numerical aperture of the condenser lens. Usually, the lateral resolution in classical dark-field microscopy is limited by the numerical aperture of the imaging part which must be smaller than the numerical aperture of the illumination part.

Results To validate the dark-field optical nanoscopy technique, a translucent object having details smaller than the diffraction limit was first placed below the microsphere. The sample, consisting of a random matrix of squares having sides of 250 nm, required two main fabrication steps: the master structure was first created by electron-beam lithography on a silicon wafer and this was then replicated by nano-imprint lithography on a glass wafer [28]. Figure 2(a) shows the direct image of the random patterns using scanning electron microscopy (SEM) which are invisible in bright-field microsphere-assisted microscopy. As for the dark-field microsphere-assisted microscope, it enables to discern the transparent square details (Fig. 2(b)). The recorded image was then compared to a numerical image (Fig. 2(d)) which was calculated by 2D convolving an estimated point spread function (PSF) (see Fig. 2(c)) with the object model [18,23,29]. The full width at half maximum of the PSF is around 200 nm (Fig. 2(e)). The intensity cross sections of both the measured and calculated super-resolution images are represented in Fig. 2(f), showing a good assessment of the PSF estimation.

To further demonstrate the imaging ability of dark-field microsphere-based nanoscopy, the QR-code-like object was then replaced by a biological sample. Figure 3(a) and (b) show the images of mouse brain axons, and in particular myelinated nerve fibres of the hippocampus, obtained

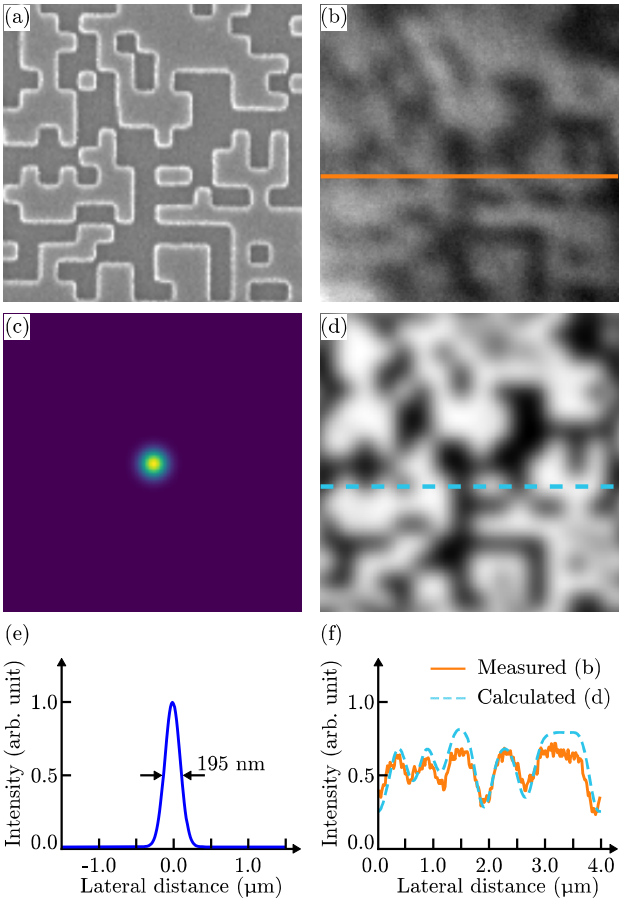

Figure 2 Dark-field super-resolution microscopy for the imaging of transparent 250-nm of side squares. (a) Image of the glass nano-imprint squares using SEM; (b) Direct image of the sample using microsphere-assisted microscopy. The soda-lime microsphere diameter is 25 µm; (c) Estimated 2D point spread function of the microsphere-based nanoscope using a Gaussian approximation; (d) Calculated image of the sample using the 2D convolution of the object model and PSF; (e) Intensity profile of PSF; (f) Intensity distribution of (b) and (d) along the transverse axis.

through a transmission electron microscope (TEM) and a bright-field microscope alone, respectively. Figure 3(c) is a zoom-in view of the direct image recorded with the optical microscope (white-dashed square in Fig. 3(b)), revealing the region of interest where the measurements were performed using the nanoscope in bright-field (Fig. 3(d)) and dark-field modes (Fig. 3(e)). It should be mentioned that, unlike conventional optical microscopy and microsphere-assisted microscopy, the examination of the sample with the TEM (at 70 kV with a magnification $\times$2000) required the preparation of the sample with a contrast enhancement solution (uranyl acetate and lead citrate). The intensity cross sections (Fig. 3(f)) demonstrates that the dark-field nanoscope not only increases the lateral resolution but also provides an enhancement of the imaging contrast. The smallest translucent cells having a size of around 300 nm are distinguished.

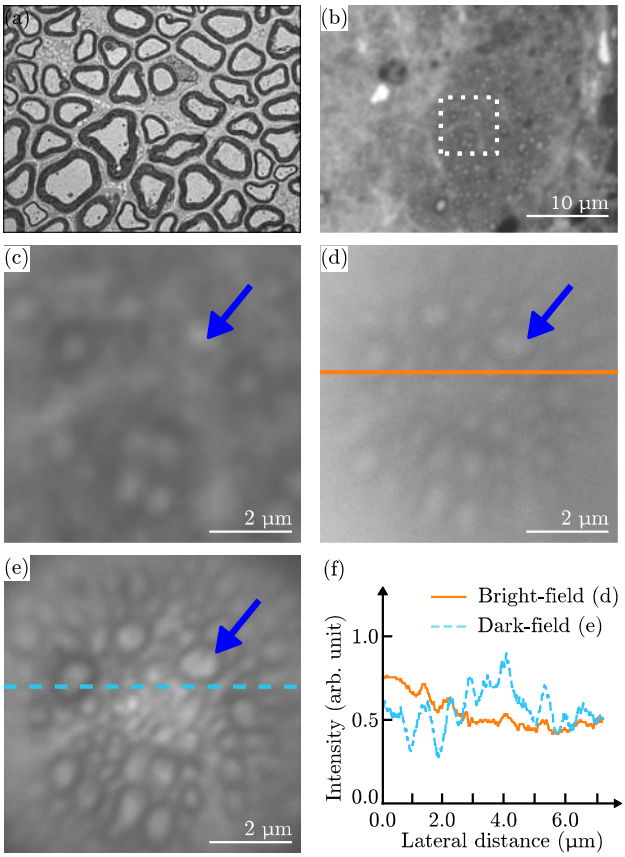

Figure 3 Dark-field super-resolution microscopy for the imaging of mouse brain cells. The myelinated nerve fibres of the hippocampus are recovered using (a) transmission electron microscopy, (b) bright-field conventional microscopy, (c) zoom-in view of (b), (d) bright-field nanoscopy and (e) dark-field nanoscopy. Arrows help for location. (f) Intensity profiles of (d) and (e) along the transverse axis.

Discussion The optical microscope is able to perform both transmission and reflection dark-field illumination of the sample. However, only the optical transmission mode proved successful for the visualisation of sub-diffraction-limit translucent objects. Indeed, in the case of dark-field reflection illumination, the presence of a central high intensity peak hinders the measurement, as shown in the example in Fig. 4(a). This effect occurs for several microsphere sizes, *i.e.* the testing of the reflective dark-field mode using bigger microspheres led to the same problem. The generation of the central bright area could be explained by the reflection of the incident conical illumination beam at the microsphere interface which is then both collected

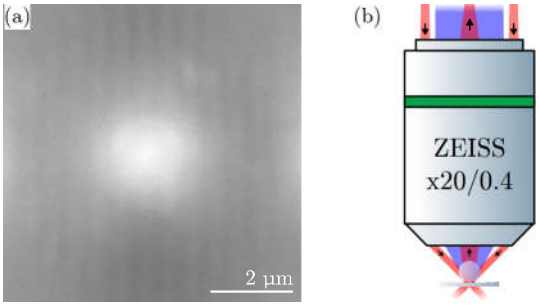

Figure 4 Dark-field microsphere-assisted microscope in the reflective mode. (a) A high intensity peak occurs in the centre of the recorded image, leading to a low imaging contrast of the object features. Here, a soda-lime microsphere was placed on a 600-nm-period positive Ronchi target. (b) Layout of the super-resolution imaging system showing the assumption of the intensity artefact generation.

by the microscope objective (see Fig. 4(b)). This artefact is not present in the transmission mode.

Conclusion A dark-field microsphere-assisted microscope has been developed for the imaging of translucent samples having feature sizes smaller than the limit imposed by the diffraction of light. The phenomenon was first characterized by measuring the transfer function of the nanoscope. Then, the imaging of glass-fabricated nanostructures and biological elements, *i.e.* brain axons, was performed. The label-free and easy-to-implement technique allows the visualization of transparent details up to 100 nm in size in air, resulting in an equivalent numerical aperture of around 1.5. The results of these imaging experiments with microsphere-assisted dark-field microscopy show that this full-field, label-free and easy-to-implement technique could be extremely interesting for many different applications in life science applications.

Acknowledgements The authors thank the French RENATECH network (FEMTO-ST institute, Besancon) for fabricating the Ronchi calibration target. This work received funding from SATT Conectus Alsace and was also supported by the University of Strasbourg and Region Grand-Est ("Soutien aux jeunes chercheurs" program). Help from the C^{3}FAB platform of ICube laboratory is also acknowledged.

References

[1] J.W. Goodman, *Introduction to Fourier optics, 3rd. Ed*, W.H. Freeman and Co Ltd, New York, USA **2004**.
[2] S. Perrin and P. Montgomery, *arXiv* **2018**, 1802.07161.
[3] Beyond the diffraction limit, *Nat. Photon.* **2009**, *3*, 361.
[4] The Nobel Prize in Chemistry 2014 - Press Release, *Nobel Media AB 2014*, Accessed: August 2018.
[5] E.H. Synge, *Phil. Mag. 7* **1928**, *6*, 356.
[6] D.W. Pohl, D. and Courjon, *Near Field Optics*, NATO ASI-E Series, Kluwer, The Netherlands **1993**.
[7] V.G. Veselago, *Sov. Phys. Usp.* **1968**, *10*, 509.
[8] J.B. Pendry, *Phys. Rev. Lett.* **2000**, *85*, 3966.
[9] X. Zhang and Z. Liu, *Nat. Mater.* **2008**, *7*, 435.
[10] W. Lukosz and M. Marchand, *Opt. Acta.* **1963**, *10*, 241.
[11] P.C. Sun and E.N. Leith, *Appl. Opt.* **1992**, *31*, 4857.
[12] M. Minsky, *US patent US3013467*, **1961**.
[13] H. Goldmann, *Ophthalmologica.* **1940**, *98*, 257.
[14] H. Naora, *Science* **1951**, *114*, 279.
[15] S.W. Hell, R. Schmidt, and A. Egner, *Nat. Photon.* **2009**, *3*, 381.
[16] Z. Chen, A. Taflove, and V. Backman, *Opt. Express* **2004**, *12*, 1214.
[17] Z. Wang, W. Guo, L. Li, B. Luk'yanchuk, A. Khan, Z. Liu, Z. Chen, and M. Hong, *Nat. Commun.* **2011**, *2*, 218.
[18] A. Darafsheh, C. Guardiola, A. Palovcak, J.C. Finlay, and A. Carabe, *Opt. Lett.* **2015**, *15*, 5.
[19] K.W. Allen, N. Farahi, Y. Li, N.I. Limberopoulos, D.E. Walker, A.M. Urbas, and V.N. Astratov, *Opt. Express* **2015**, *23*, 24484.
[20] Y. Ben-Aryeh, *J. Opt. Soc. Am. A* **2016**, *33*, 2284.
[21] A. Darafsheh, N.I. Limberopoulos, J.S. Derov, D.E. Walker Jr., and V.N. Astratov, *Appl. Phys. Lett.* **2014**, *104*, 061117.
[22] H. Yang, N. Moullan, J. Auwerx, and M.A.M. Gijs, *Small* **2014**, *10*, 1712.
[23] A. Brettin, C.L. McGinnis, K.F. Blanchette, Y.E. Nesmelov, N.I. Limberopoulos, D.E. Walker, A.M. Urbas, and V.N. Astratov, in *National Aerospace and Electronics Conference*, IEEE, Dayton, USA **2017**, pp. 189-192.
[24] A. Leong-Hoi, C. Hairaye, S. Perrin, S. Lecler, P. Pfeiffer, and P. Montgomery, *Phys. Status Solidi A* **2017**, *215*, 1700858.
[25] I. Kassamakov, S. Lecler, A. Nolvi, A. Leong-Hoi, P. Montgomery, and E. Haeggstrom, *Sci. Rep.* **2017**, *7*, 3683.
[26] S. Perrin, A. Leong-Hoi, S. Lecler, P. Pfeiffer, I. Kassamakov, A. Nolvi, E. Haeggstrom, and P. Montgomery, *Appl. Opt.* **2017**, *56*, 7249.
[27] Y. Zhou, Y. Tang, Q. Deng, L. Zhao, and S. Hu, *Appl. Phys. Express* **2017**, *10*, 082501.
[28] G. Quaranta , G. Basset, O.J.F. Martin, and B. Gallinet, *ACS Photonics* **2017** *4*, 1060.
[29] W.V. Houston, *Astrophys. J.* **1926**, *64*, 81.

Graphical Table of Contents

Imaging of sub-diffraction-limit transparent objects is presented using dark-field optical nanoscopy (DFN). Based on microsphere-assisted microscopy, the resolving power of the label-free super-resolution system allows the visualization of not only translucent features having a size of at least 200 nm, but also biological elements. This makes DFN extremely interesting for life science applications.